Electronic Supplementary Information (ESI)

Molecular insights into the Patched 1 drug efflux inhibitory activity of Panicein A Hydroquinone: a computational study

Sandra Kovachka [a, b], Giuliano Malloci *[c], Attilio Vittorio Vargiu [c], Stéphane Azoulay [a], Isabelle Mus-Veteau *[b] and Paolo Ruggerone [c]

[a] *Université Côte d'Azur, CNRS, ICN, 28 Avenue Valrose, 06108 Nice, CEDEX 2, France;*

[b] *Université Côte d'Azur, CNRS, IPMC, 660 Route des Lucioles, 06560 Valbonne, France;*

[c] *Dipartimento di Fisica, Università di Cagliari, Cittadella Universitaria, I-09042 Monserrato (CA), Italy.*

	E-PAH	Z-PAH	S-PAH	R-PAH	E-PA	Z-PA	E-*m*OMe	Z-*m*OMe
Chemical Formula	$C_{22}H_{28}O_3$	$C_{22}H_{28}O_3$	$C_{22}H_{30}O_3$	$C_{22}H_{30}O_3$	$C_{22}H_{26}O_3$	$C_{22}H_{26}O_3$	$C_{23}H_{30}O_3$	$C_{23}H_{30}O_3$
Molecular Weight	340.46	340.46	342.48	342.48	338.45	338.45	354.49	354.49
Atoms; Heavy atoms	53; 25	53; 25	55; 25	55; 25	51; 25	51; 25	56; 26	56; 26
Rotatable Bonds	13	13	14	14	11	11	14	14
H bonds donors/acceptors	2 / 3	2 / 3	2 / 3	2 / 3	0 / 3	0 / 3	3 / 1	3 / 1
LogP	6.50	6.50	6.91	6.91	6.04	6.04	6.65	6.65
LogS	-5.59	-5.59	-6.09	-6.09	-6.81	-6.81	-5.99	-5.99
Molecular Surface Area (A^2)	563.44	563.31	586.42	586.40	531.69	531.82	600.43	600.64
Van der Waals Volume (A^3)	343.35	343.38	349.34	349.31	338.43	338.43	360.60	360.61

Table S1. Comparison between computed molecular descriptors of PAH and its derivatives considered in this study.

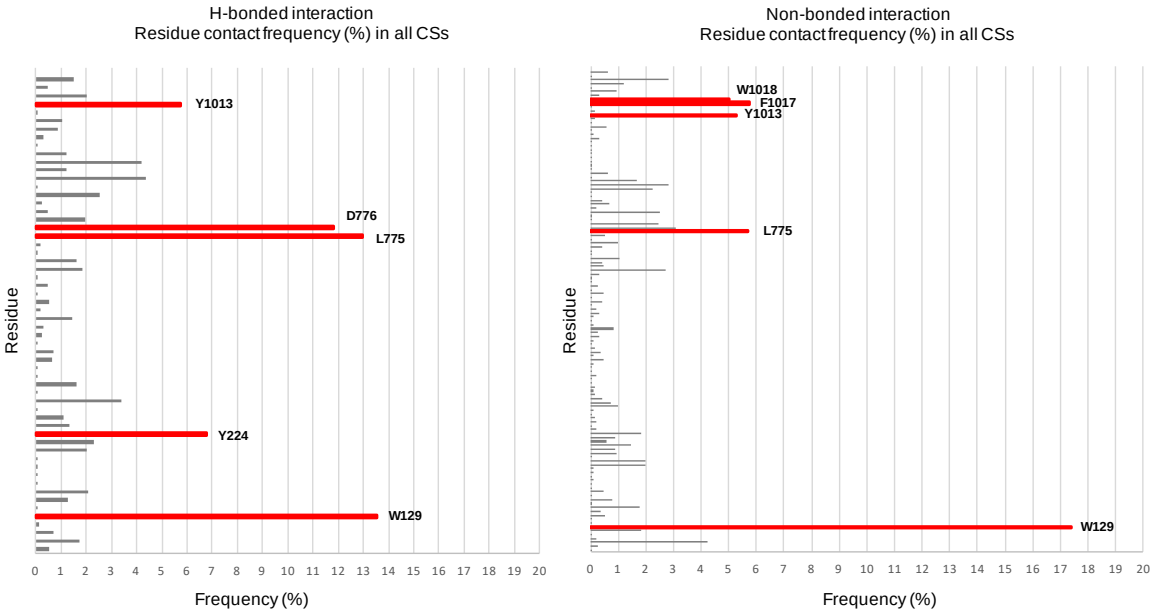

Figure S1. FTMap contact analysis: contact frequency per residue: most relevant residues with contact frequency >5% are highlighted in red and labelled, all other are represented in grey.

Ligand dynamics in water solution

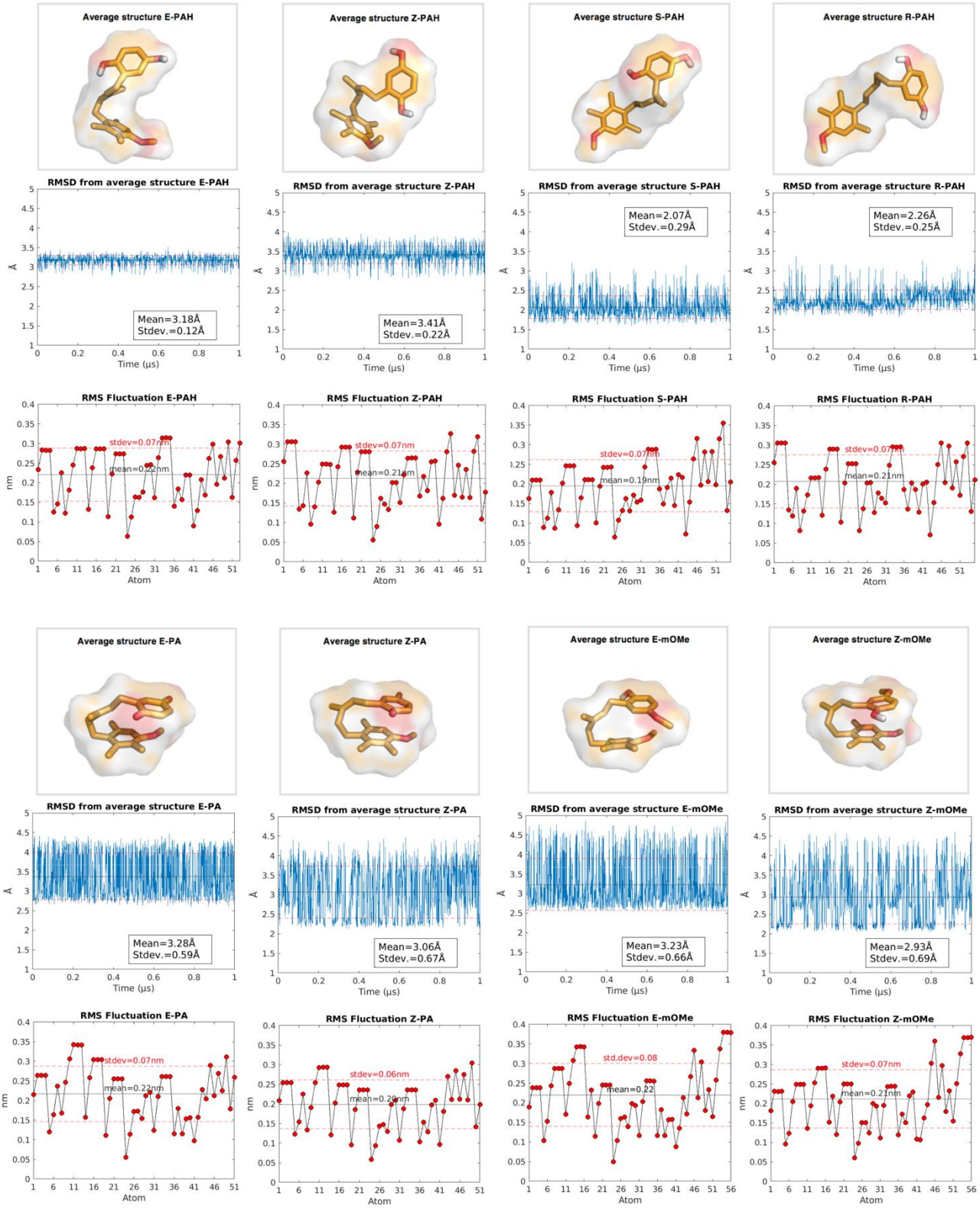

Figure S2. Average structures during MD simulation, RMSD and RMSF graphs extracted from 1 μs-long MD simulation in water for E-PAH, Z-PAH, S-PAH, R-PAH, E-PA, Z-PA, E-mOMe and Z-mOMe.

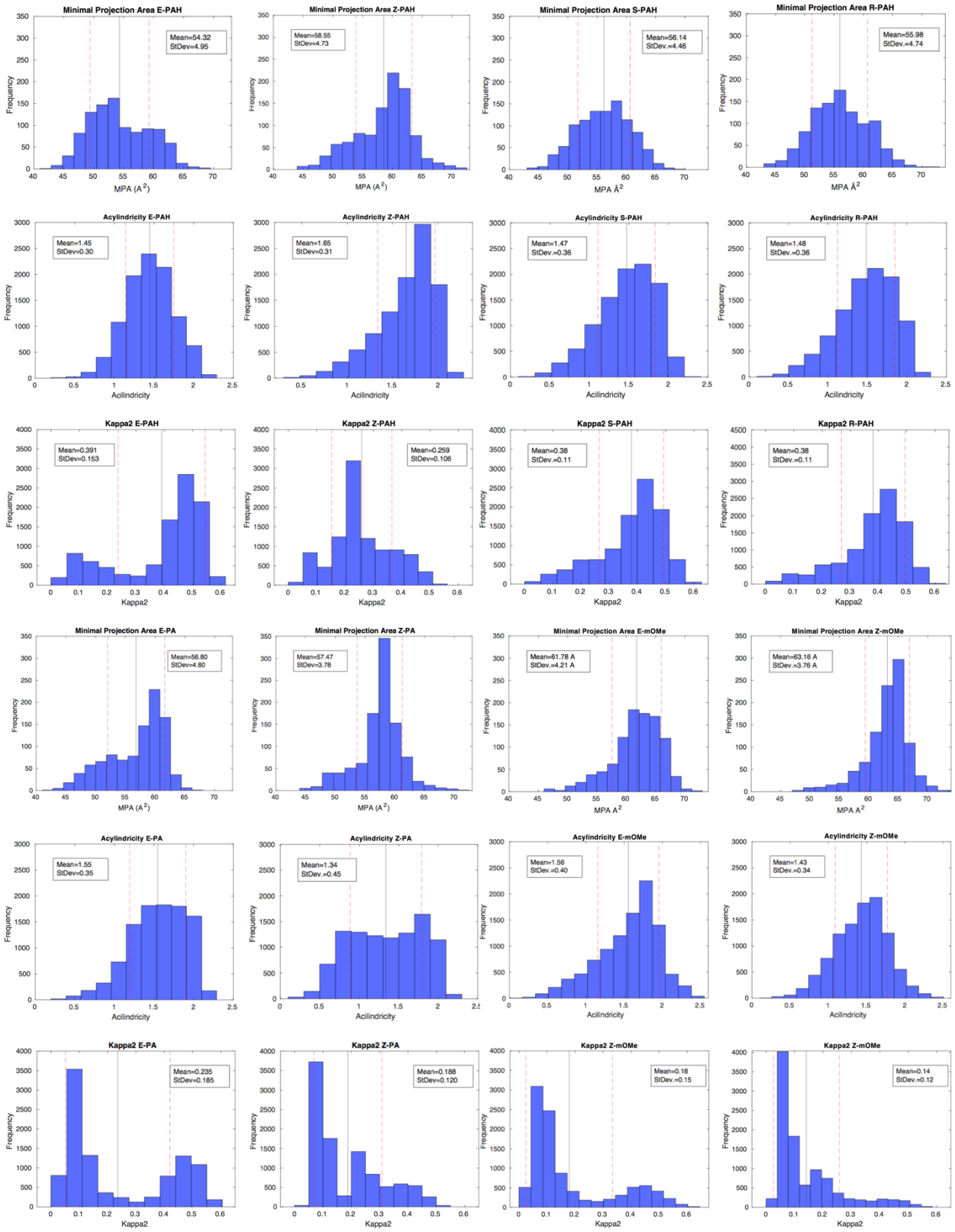

Figure S3. Morphology descriptors Minimal Projection Area, Acylindriciy and Kappa2 graphs extracted from 1 µs-long MD simulation in water for E-PAH, Z-PAH, S-PAH, R-PAH, E-PA, Z-PA, E-mOMe and Z-mOMe.

Cholesterol redocking – Method validation

Ligand	Cluster	Custer population (µs of MD)	Ligand conformation	Number of poses within the Neck pocket	Number of poses within the ECD pocket 1
Cholesterol	C1	0.390	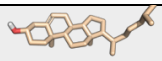	16	1
	C2	0.369	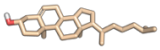	15	3
	C3	0.103	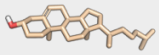	16	2
	C4	0.092	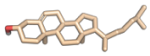	16	3
	C5	0.017	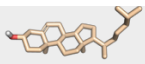	11	2
	C6	0.016	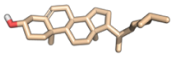	11	0
	C7	0.010	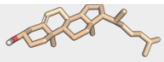	8	5
	C8	0.002	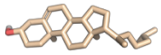	13	5
	C9	0.002	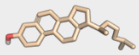	12	5
	C10	0.001		15	2

Table S2. Cluster population and representative conformations used in ensemble docking of cholesterol. The number of docking poses within the 2 main pockets, Neck Pocket and ECD Pocket 1 are indicated.

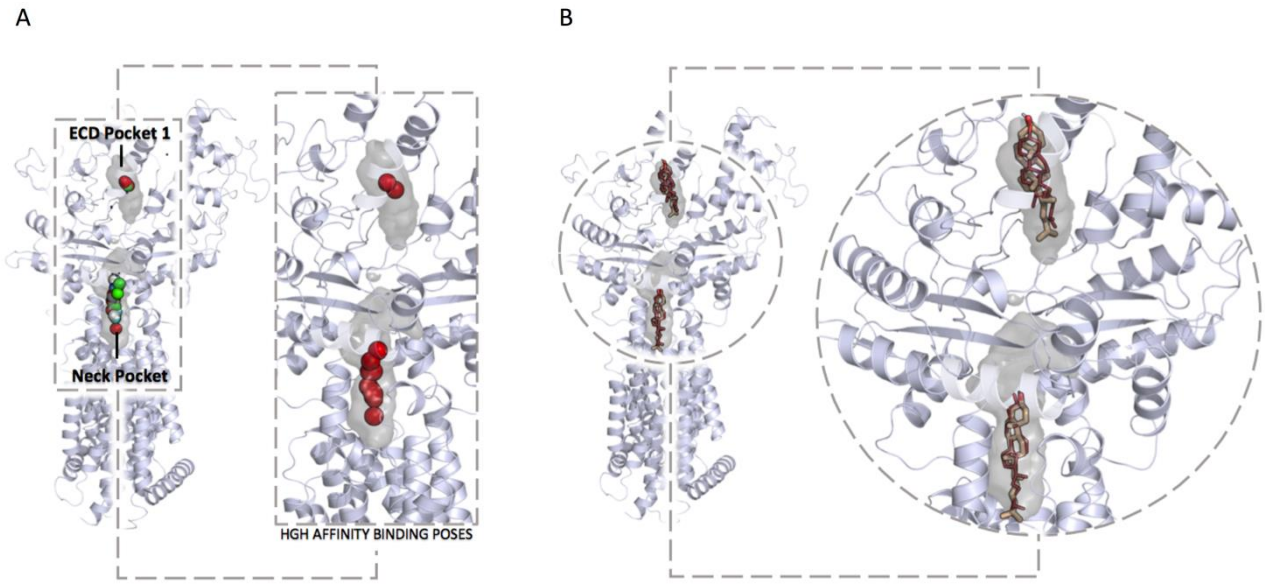

Figure S4. A) Docking poses distribution on the protein surface for the inhibitors. The surface of the two pockets is represented in grey. The centers of mass of the docked poses are represented as spheres with radius increasing with the cluster population and colored according to the binding affinity with the following color-code: > -10.5 kcal/mol, blue; [-10.5, -11.0] kcal/mol, cyan; [-11.0, -11.5] kcal/mol, green; [-11.5, -12.0] kcal/mol, white; ≤–12.0 kcal/mol, red; B) Cryo-EM (PDB ID 6n7h) cholesterol binding mode and docking pose superimposition are shown in firebrick and wheat color respectively. The binding affinities of cholesterol for the ECD and Neck binding pocket are -12.1 kcal/mol and -12.2 kcal/mol respectively and the docked conformation belongs to the second most populated cluster C2, conformation assumed for 37% of the simulation time.

Blind Ensemble Docking

Conformations employed in docking with Autodock VINA

Ligand	Cluster	Custer population (μs of MD)	Ligand conformation	Number of poses within the Neck pocket	Number of poses within the ECD pocket 1
E-PAH	C1	0.198	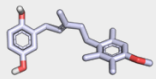	13	3
	C2	0.194	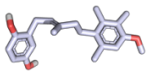	13	1
	C3	0.176	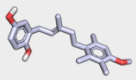	10	3
	C4	0.158	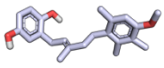	12	0
	C5	0.107		3	0
	C6	0.093		3	0
	C7	0.022	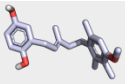	8	2
	C8	0.021	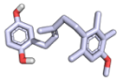	14	2
	C9	0.017	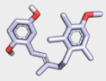	6	0
	C10	0.015	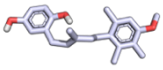	13	3
Z-PAH	C1	0.286	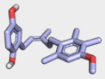	11	0
	C2	0.238	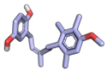	7	0
	C3	0.114	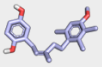	13	1
	C4	0.079	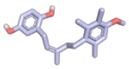	12	2
	C5	0.079	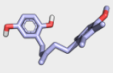	13	0
	C6	0.058	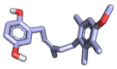	10	1
	C7	0.049	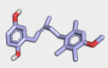	11	0
	C8	0.045	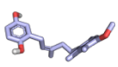	11	0
	C9	0.032	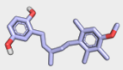	10	1
	C10	0.020	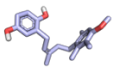	11	0

S-PAH	C1	0.237	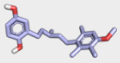	14	0
	C2	0.223	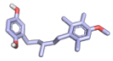	14	1
	C3	0.184		8	1
	C4	0.103	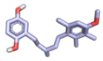	11	2
	C5	0.093	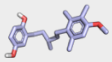	12	0
	C6	0.070	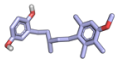	15	0
	C7	0.032		1	0
	C8	0.032		6	0
	C9	0.018		10	3
	C10	0.008	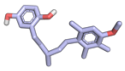	9	1
R-PAH	C1	0.263	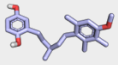	11	2
	C2	0.222	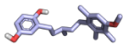	12	0
	C3	0.168	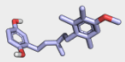	12	4
	C4	0.137	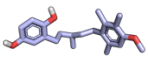	13	0
	C5	0.064	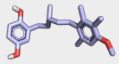	10	2
	C6	0.055	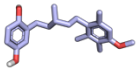	11	2
	C7	0.039		4	0
	C8	0.025		13	1
	C9	0.017		3	1
	C10	0.010	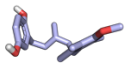	9	1

Table S2. Cluster population and conformations along with number of poses docked within the Neck and ECD binding pocket during ensemble blind docking for E-PAH, Z-PAH, S-PAH and R-PAH.

Ligand	Cluster	Custer population (μs of MD)	Ligand conformation	Number of poses within the Neck pocket	Number of poses within the ECD pocket 1
E-PA	C1	0.311		4	1
	C2	0.273		3	1
	C3	0.099	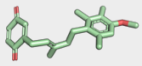	13	1
	C4	0.080	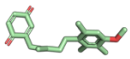	10	1
	C5	0.074	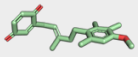	11	2
	C6	0.062	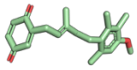	8	2
	C7	0.050	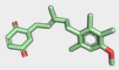	8	2
	C8	0.032	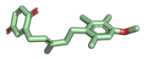	14	5
	C9	0.011	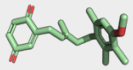	14	1
	C10	0.010	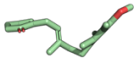	12	0
Z-PA	C1	0.431		1	2
	C2	0.215	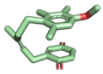	2	0
	C3	0.077	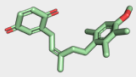	12	0
	C4	0.047	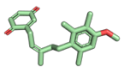	9	2
	C5	0.044	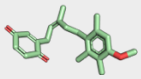	9	1
	C6	0.041		14	1
	C7	0.041	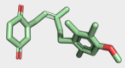	13	3
	C8	0.037	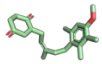	10	0
	C9	0.034	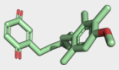	13	2
	C10	0.033	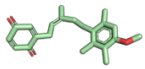	13	2

E-*m*OMe	C1	0.350		2	0
	C2	0.332		0	0
	C3	0.070	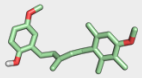	12	0
	C4	0.065	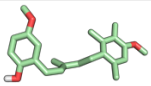	10	1
	C5	0.044	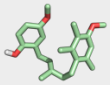	6	0
	C6	0.042	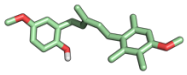	12	3
	C7	0.040	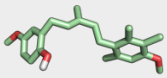	12	1
	C8	0.028	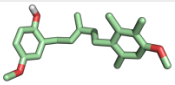	10	1
	C9	0.015	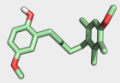	14	0
	C10	0.014	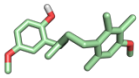	6	2
Z-*m*OMe	C1	0.429	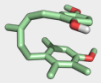	1	1
	C2	0.284	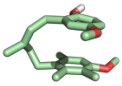	0	0
	C3	0.066	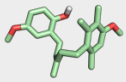	9	0
	C4	0.058	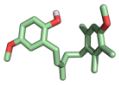	11	0
	C5	0.038	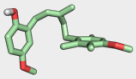	13	1
	C6	0.031	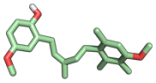	8	0
	C7	0.028	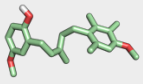	11	1
	C8	0.025	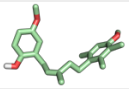	10	0
	C9	0.024	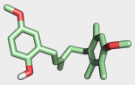	7	0
	C10	0.017	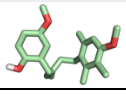	6	0

Table S3. Cluster population and conformations along with number of poses docked within the Neck and ECD binding pocket during ensemble blind docking for E-PA, Z-PA, E-*m*OMe and Z-*m*OMe.

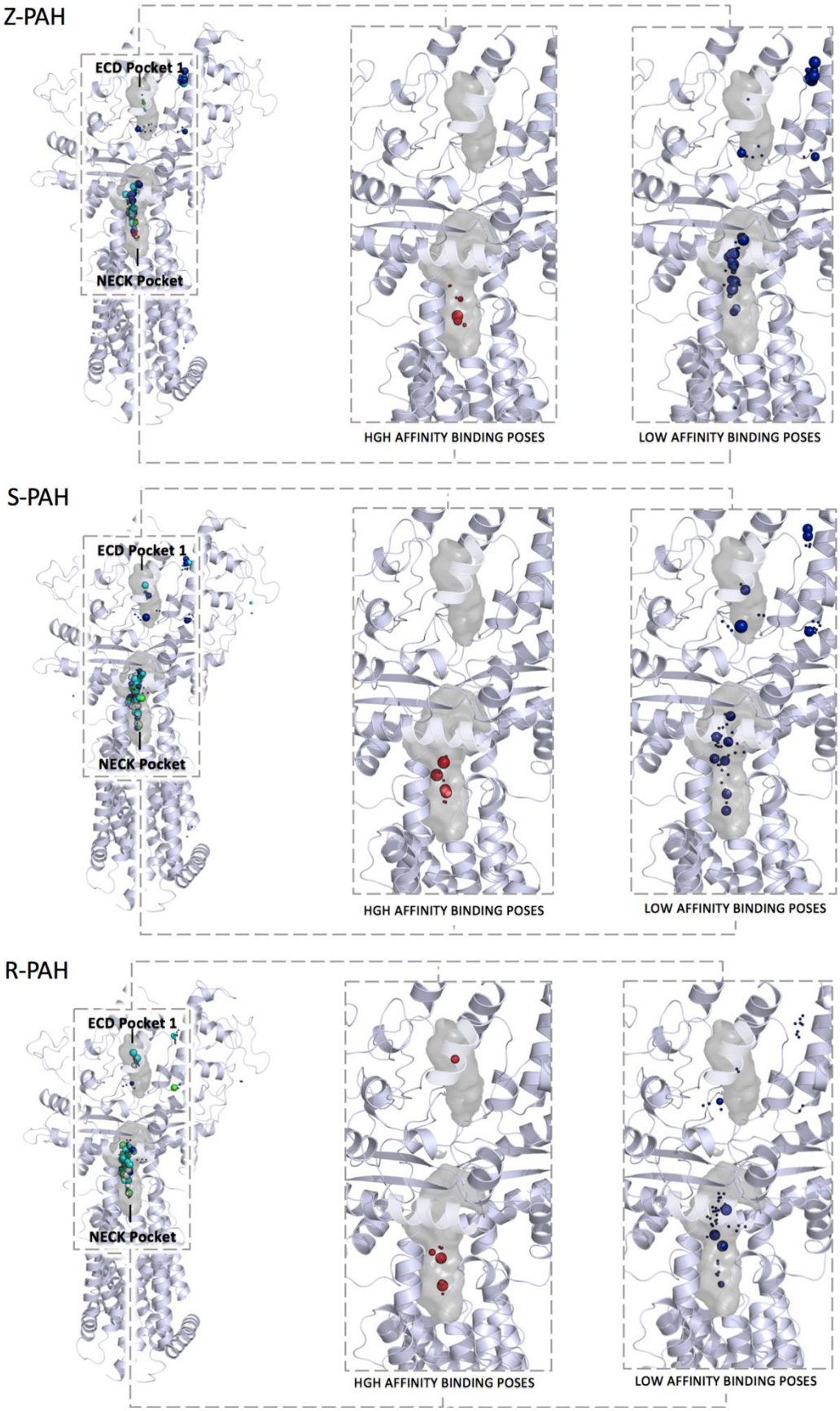

Figure S5. Docking poses distribution on the protein surface for Z-PAH, S-PAH and R-PAH. The surface of the two pockets is represented in grey. The centers of mass of the docked poses are represented as spheres with radius increasing with the cluster population and colored according to the binding affinity with the following color-code: > -9.0 kcal/mol, blue; [-9.0, -9.5] kcal/mol, cyan; [-9.5, -10.0] kcal/mol, green; [-10.0,-10.5] kcal/mol, white; ≤−10.5 kcal/mol, red.

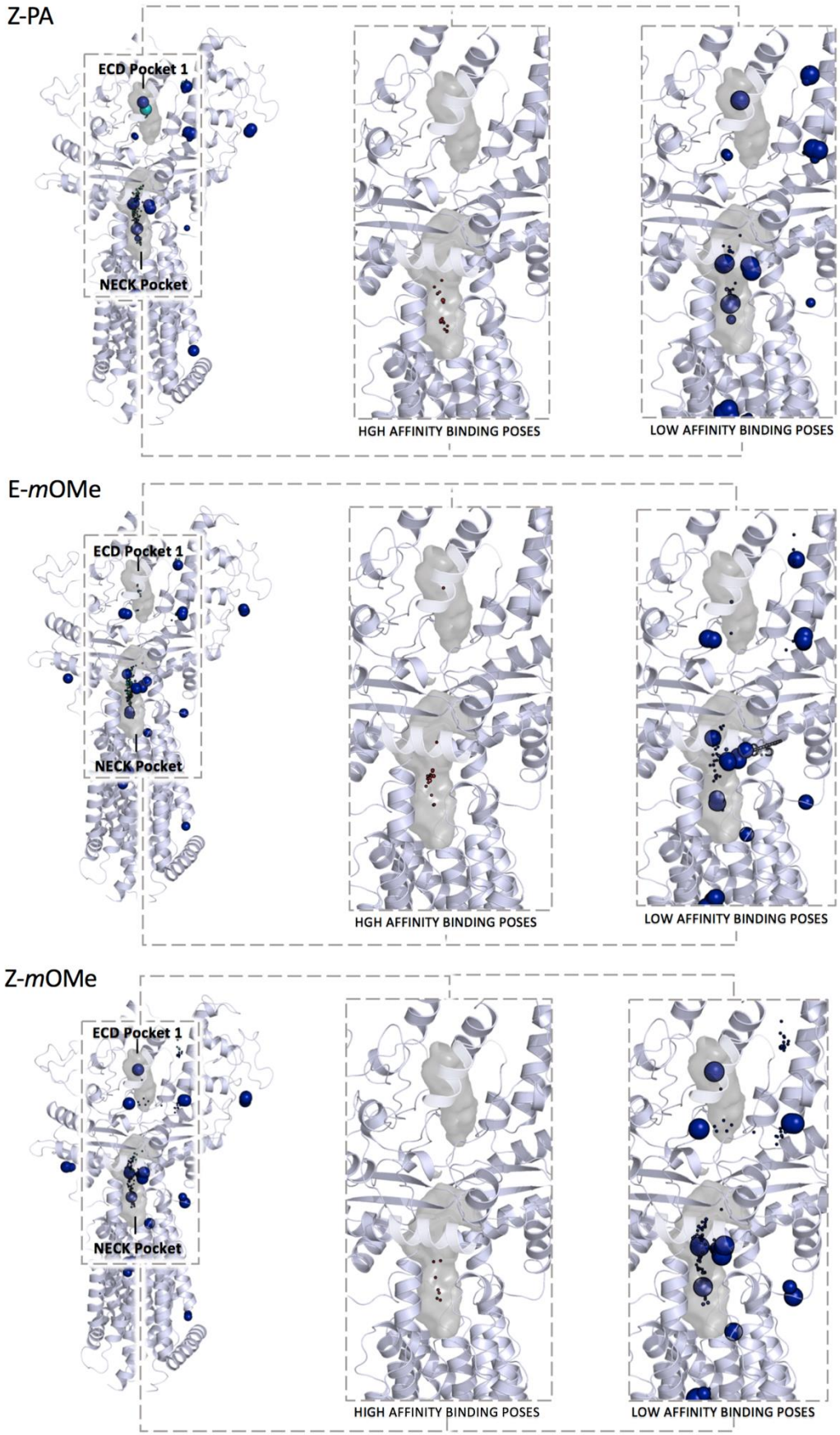

Figure S6. Docking poses distribution on the protein surface for Z-PA, E-*m*OMe and Z*m*OMe. The surface of the two pockets is represented in grey. The centers of mass of the docked poses are represented as spheres with radius increasing with the cluster population and colored according to the binding affinity with the following color-code: > -9.0 kcal/mol, blue; [-9.0, -9.5] kcal/mol, cyan; [-9.5, -10.0] kcal/mol, green; [-10.0,-10.5] kcal/mol, white; ≤−10.5 kcal/mol, red.